

Determination of the Production Rate and Cumulative Production in the “No Flow” Boundary Condition Utilizing the Finite Element Method

Blessing Otamere* and Iredia Davis Erhunmwun**

Dr., Department of Petroleum, Faculty of Engineering, University of Benin, Benin City, Nigeria.
E-mail: blessing.otamere@uniben.edu ORCID: 0009-0004-8606-1388

Prof., Department of Production, Faculty of Engineering, University of Benin, Benin City, Nigeria.
E-mail: iredia.erhunmwun@uniben.edu ORCID: 0000-0002-0497-8220

Corresponding Author: E-mail: blessing.otamere@uniben.edu ORCID: 0009-0004-8606-1388

Received: 11.12.2025 Accepted: 09.02.2026

Abstract - The No Flow outer boundary condition also known as the **PSEUDO-STEADY STATE (PSS)** occurs when reservoirs outside boundary lines are all closed boundaries in the late time region. This condition is relevant to bounded reservoirs. In this research, we employed the well the rate of production and cumulative production in a circular reservoir adopting the Finite Element Method (FEM). The FEM was used to analyze the diffusivity equation (governing equation). The reservoir was divided into fragments, which is referred to finite element. These components were examined and then put together to create the reservoir's domain. The research was conducted under the presumption that the pressure in the reservoir was uniformly distributed prior to the well starting production. Due to the nature of the diffusivity equation, dimensional analysis was carried out to make the equation dimensionless. The dimensionless results indicate a linear increase in cumulative production over time. Thereafter, the dimensionless cumulative production becomes asymptotically constant with a very slight increase as the dimensionless time increases. This continues throughout this flow regime. The results indicate a decline in the production rate of the reservoir over time. The rate of decrease at the initial stage is high and later in the regime, becomes steady. The finding of this study was juxtaposed with the obtained results of Christine. The comparison reveals that the two approaches have a high positive correlation, with an overall percentage error of 1.5512 & 0.0891 and a minimal percentage error of 0.0001 & 0.0111 produces the dimensionless cumulative production & the dimensionless production rate, respectively. Again, Christine solutions only stated the reservoir's production rate and cumulative production at certain times, but this work estimates the reservoir's overall production rate and cumulative output simultaneously.

Keywords: Equation of diffusivity, No Flow boundary, cumulative production, production rate

1. Introduction

In a bid to accurately anticipate the behaviours of compressible and incompressible fluids, physicists, engineers, and hydrologists have showed a keen delight in the flow of fluid in reservoirs or porous medium. To verify the application of their suggested correlations, they established a number of investigations [1, 12, 14]. The diffusivity equation is the fundamental formula for determining the pressure distribution in a reservoir. For this equation, it has been assumed that the reservoir temperature will be constant, which is usually a reasonable assumption.

To solve the diffusivity equation, a number of techniques have been put forth, including analytical and numerical ones. [13], [2, 15] solved the diffusivity equation using the Laplace transformation. This technique converts the partial differential equations into an analytically solvable system of ordinary differential equations [17]. The solution obtained for the Laplace transform of the pressure $\overline{p_D}$, was a function of the Laplace parameter ℓ & the spacial parameter, r_D . To determine the pressure ℓ as a function of r_D and t_D , the Laplace space solutions must be inverted using the inverse Laplace transformation [16].

A dimensionless solution to the diffusivity equation has been found [3]. The impact of ignoring the quadratic gradient factor on solving the diffusion equation governing the transient state were quantitatively analysed in [4]. It should be mentioned that out of all the flow regimes in the reservoir, the transient flow was the most essential state that allowed for the determination of vital characteristics including permeability, reservoir capacity, and skin factor through well test analysis [5-6, 18].

Braeuning, Jelmert, and Vik's study, which used the modified logarithm transform to solve the diffusivity equation, is another intriguing example in this area. In their solution, they took wellbore storage and skin damage into consideration. They observed that the wellbore damage, pseudo-skin from partial penetration, and non-linear low parameter all affect the amount of inaccuracy resulting from linearisation of the diffusivity equation. [7]. Another instance is when Dusseault and Wang utilised the Laplace transform to solve the non-linear diffusivity problem analytically. They asserted that the large pressure gradient, the core's compressibility, and the injected fluids were the causes of the observed departure of their method from current solutions [8]. The pressure drop profile along the reservoir's radius may change as a result of these approximations and considerations, whether or not these changes are significant.

[9, 19] demonstrated how to create a general analytical solution for the multidimensional hydraulic diffusivity problem using the integral transform technique. The proposed method maximised the application of superposition theory by directly addressing time-related well rates and boundary conditions.

Some researchers developed a generalised mathematical framework model and numerical method for simulating unconventional gas reservoirs [10, 21]. Generalised flow models with random grids served as the foundation for both the model and the numerical method.

In order to determine the significant physical characteristics of the reservoir that affect the pressure drops, a thorough sensitivity analysis was conducted after comparing the analytical and numerical solutions for both linear and nonlinear diffusivity equations performed at wellbore radius. [11, 20] In an effort to determine where the pressure differences of the linear and nonlinear diffusivity equations were important, they also carefully looked at variables including depletion time, reservoir radius, and production rate.

This investigation is necessary since none of the x-rayed techniques have been able to thoroughly analyse the dimensionless cumulative output and production rate.

The aim of this study is to develop a finite element based numerical framework for solving the radial diffusivity equation in a bounded circular reservoir operating under a no-flow (pseudo-steady state) boundary condition, with emphasis on evaluating reservoir production performance.

The study seeks to evaluate the dimensionless production rate and cumulative production of the reservoir over a wide range of dimensionless times and radii, to analyse the production decline behaviour and cumulative production trends characteristic of the pseudo steady state flow regime, and to validate the numerical results through comparison with established solutions reported in the literature, particularly those of Christine [], using percentage error analysis.

2. Methodology

The properties of the flow in a circular reservoir can be ascertained using the diffusivity equation. Equation 1 is shown below.

$$\frac{\partial^2 P_D}{\partial r_D^2} + \frac{1}{r_D} \frac{\partial P_D}{\partial r_D} = \frac{\partial P_D}{\partial t_D} \quad (1)$$

The numerically solution was solved using the finite element method under the assumption of radial symmetry. The physical domain of interest extends from the wellbore radius $r = r_w$ to the external reservoir radius $r = r_e$, where production is influenced by a closed outer boundary.

At the **inner boundary** a constant production rate was prescribed at the wellbore. This corresponds to a Neumann type boundary condition expressed mathematically as

$$-kh \frac{\partial p}{\partial r} /_{r=r_w} = qu$$

which enforces a fixed flux into the well. At the **outer boundary**, a no flow (closed) condition was imposed, given by

$$\frac{\partial p}{\partial r} /_{r=r_e} = 0$$

This condition implies that no fluid crosses the reservoir boundary and is the characteristic of pseudo steady state flow in bounded reservoirs.

The reservoir domain was discretized using a one-dimensional radial finite element mesh of about **80 nonuniform elements**. Mesh refinement was applied near the wellbore to capture steep pressure gradients, while coarser elements were used toward the no flow outer boundary. Quadratic interpolation ensured stable solutions with convergence errors of order 10^{-4} . Time integration

was performed using the **Crank Nicolson scheme** with variable time stepping. Smaller time steps were used at early simulation times, while progressively larger steps were adopted at late times to efficiently reach dimensionless times up to 10^6

As a result, the boundary as well as initial conditions will become:

1. Dimensionless initial condition:

The reservoir's uniform pressure

$$P_D(r_D, t_D = 0) \leq 0 \quad (2)$$

2. Dimensionless Internal Boundary Condition:

The constant rate at the well

$$\frac{\partial P_D}{\partial r_D}(1, t_D) = 1 \quad (3)$$

3. Dimensionless Outer Boundary Conditions:

- a. "Infinite Acting" Reservoirs

No reservoir boundary

$$P_D(r_D \rightarrow \infty, t_D) = 0 \quad (4)$$

- b. "No Flow" boundary:

There's no influx across the reservoir

$$\frac{\partial P_D}{\partial r_D}(r_{eD}, t_D) = 0 \quad (5)$$

- c. Boundary of Constant Pressure:

outer boundary of constant pressure

$$P_D(r_{eD}, t_D) = 0 \quad (6)$$

Eq. 1 can alternatively be presented in a shorten version as:

$$\frac{1}{r_D} \frac{\partial}{\partial r_D} \left(r_D \frac{\partial P_D}{\partial r_D} \right) = \frac{\partial P_D}{\partial t_D} \quad (7)$$

The governing equation can only be calculated if it is in order one in the evaluation using the Finite Element method. However, because its governing equation is of order two, the diffusivity equation must be modified to order one. The interpolation functions that enable us to build the finite element model are then introduced. The elements matrices are produced using this model, which is then put together to depict the reservoir's full domain. Although the assembled matrix cannot be solved explicitly, the nodal values of the variable can be found by adding either the initial conditions or the boundary condition, or a combination of the two. The following methods were applied& eq. 7 becomes:

$$K [K_{ij}^e] \{P_D\} + [M_{ij}^e] \left\{ \dot{P}_{Dj} \right\} = \{Q_i^e\} \quad (8)$$

The generated finite element model in Equation 8 represents the diffusivity equation in the unsteady state flow regime. in which,

$$K_{ij}^e = \int_{r_{DA}}^{r_{DB}} r_D \frac{d\psi_i^e}{dr_D} \frac{d\psi_j^e}{dr_D} dr_D \quad (9)$$

$$M_{ij}^e = \int_{r_{DA}}^{r_{DB}} r_D \psi_i^e \psi_j^e dr_D \quad (10)$$

Applying Lagrange interpolation functions with a quadratic component:

$$\psi_1(r_D) = \frac{1}{h_e^2} (h_e + r_{DA} - r_D) (h_e - 2r_D + 2r_{DA}) \quad (11)$$

$$\psi_2(r_D) = \frac{4}{h_e^2} (r_D - r_{DA}) (h_e + r_{DA} - r_D) \quad (12)$$

$$\psi_3(r_D) = \frac{-1}{h_e^2} (r_D - r_{DA}) (h_e - 2r_D + 2r_{DA}) \quad (13)$$

Table 1. List of Symbols

Symbol	Parameter Description	Unit
P	Reservoir pressure	Pa
p_i	Initial reservoir pressure	Pa
p_w	Wellbore pressure	Pa
r_w	Wellbore radius	M
r	Radial distance from the wellbore	M
T	time	S
A	Diffusivity coefficient	m ² /s
ϕ	Porosity of the reservoir	
c_t	Total compressibility of rock fluid system	Pa ⁻¹
q	Constant production rate at the well	m ³ /s
μ	Fluid viscosity	PaS
h	Reservoir thickness	M
k	Absolute permeability of the reservoir	m ²
r_D	Dimensionless radius	
p_D	Dimensionless pressure	
q_D	Dimensionless production rate	
N_{PD}	Dimensionless cumulative production	
θ	Time weighting factor (Crank Nicolson scheme)	
s	Time step	

2.1 Time approximation for Conductive Heat Transfer Model

We convert the ordinary differential equation in time to an algebraic equation because the problem is time-dependent. The most popular approach is the α interpolation family. This can be achieved by utilising linear interpolations of the values of the variables of the two consecutive time steps to approximate a weighted average of the time derivative of the dependent variable.

For a given time, step s , eq. 8 becomes:

$$\{P_D\}_s + [M_{ij}^\theta]\{\dot{P}_D\}_s = \{Q_i^\theta\}_s \quad (14)$$

After the subsequent time step $s+1$, eq. 8 becomes

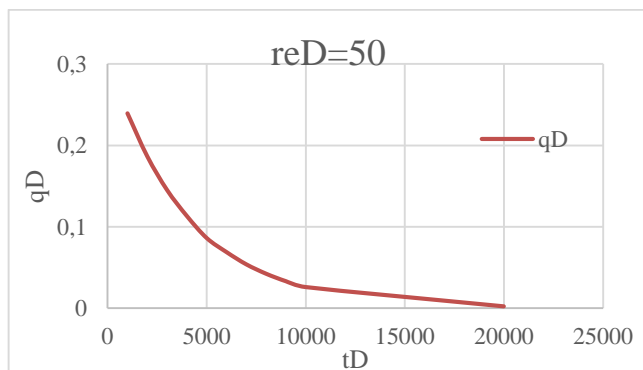
$$[K_{ij}^\theta]\{P_D\}_{s+1} + [M_{ij}^\theta]\{\dot{P}_D\}_{s+1} = \{Q_i^\theta\}_{s+1} \quad (15)$$

After multiplying eq. 14 and eq. 15 by $(1-\alpha)$ and α , adding the two resulting equations, we obtain

$$M_{ij}^\theta[(1-\alpha)\{\dot{P}_D\}_s + \alpha\{\dot{P}_D\}_{s+1}] + [K_{ij}^\theta][(1-\alpha)\{P_D\}_s + \alpha\{P_D\}_{s+1}] = \{Q_i^\theta\}_s + \alpha\{Q_i^\theta\}_{s+1} \quad (16)$$

3. Results and Discussion

The PSEUDO-STEADY STATE (PSS) is another name for this case. This occurred at the late-time-region when the external-boundary of the reservoir are all closed boundaries. Bounded reservoirs are relevant to the condition under consideration. This is to show that the reservoir has been producing long enough for the exterior boundary to feel the impact of the disturbance that was started in the reservoir. In that case, the rate at which the effect moves through the reservoir may be affected by the geometry of the drainage area or the effects of the reservoir boundaries. As a result, it is believed that the well acts as though a solid "brick wall" surrounds its external boundary, preventing fluids from entering the reservoir's radial cell. This "brick wall" could take the form of a fault that causes a significant degree of anisotropy or a change in the permeability of the reservoir walls. This may occur not only when sealing faults occur at the reservoir boundaries but also when no-flow boundaries are caused by adjacent producing.



The α interpolation family for consideration of time is given as:

$$(1-\alpha)\{\dot{P}_D\}_s + \alpha\{\dot{P}_D\}_{s+1} = \frac{\{P_D\}_{s+1} - \{P_D\}_s}{\Delta t_{s+1}} \quad (17)$$

Using the Crank-Nicholson function, substitute equation 17 in equation 16, where $\alpha = 1/2$,

$$[M_{ij}^\theta + \frac{\Delta t_{s+1}}{2} K_{ij}^\theta]\{P_D\}_{s+1} = [M_{ij}^\theta - \frac{\Delta t_{s+1}}{2} K_{ij}^\theta]\{P_D\}_s + \frac{\Delta t_{s+1}}{2} [\{Q_i^\theta\}_s + \{Q_i^\theta\}_{s+1}] \quad (18)$$

When initial Substituting the initial condition, we have:

$$Q_i = \left[\frac{1}{\Delta t_1} [M_{ij}] + \frac{1}{2} K_{ij}^\theta \right] \{P_{Dj}\}_1 - \left[\frac{1}{\Delta t_1} [M_{ij}] - \frac{1}{2} K_{ij}^\theta \right] \{P_{Dj}\}_0 \quad (19)$$

Throughout this flow regime, the reservoir functions as a tank. throughout the reservoir, the pressure declines at the same steady rate. Thus, at an external boundary, in line with Darcy's law,

$$\frac{\partial P}{\partial r} = 0 \text{ at } r = r_{eD}$$

Furthermore, if the well produces at a constant flow rate, the cell pressure will decrease in a way that $\frac{\partial P}{\partial t} \approx \text{constant}$, $\forall r$ and t .

To ascertain the pore volume, the pseudo steady state flow data must be analysed. V_p of the reservoir and also the initial hydrocarbon in place.

Graphs of dimensionless production rate against dimensionless time have been used to display the analysis's findings. These are represented in Figures. 1 to 13. These were displayed for various radial values of dimensionless times and radii.

Figure 1. A graph of q_D versus t_D at $r_{eD} = 50$. under "Closed" boundary condition

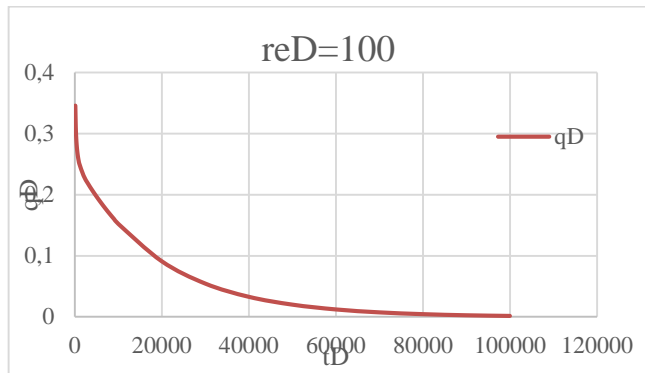


Figure 2. A graph of q_D versus t_D at $r_{eD} = 100$ under “Closed” boundary condition

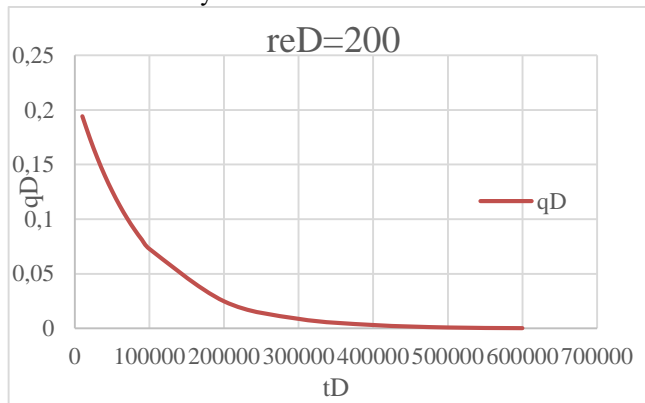


Figure 3. A graph of q_D versus t_D at $r_{eD} = 200$ under “Closed” boundary condition

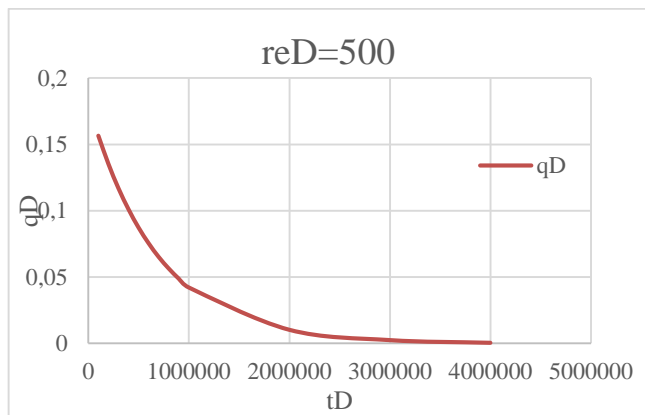


Figure 4. A graph of q_D versus t_D at $r_{eD} = 500$. under “Closed” boundary condition

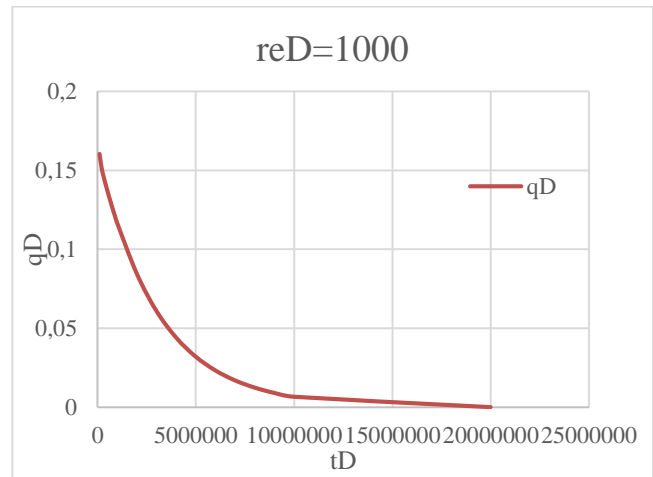


Figure 5. A graph of q_D versus t_D at $r_{eD} = 1000$. under “Closed” boundary condition

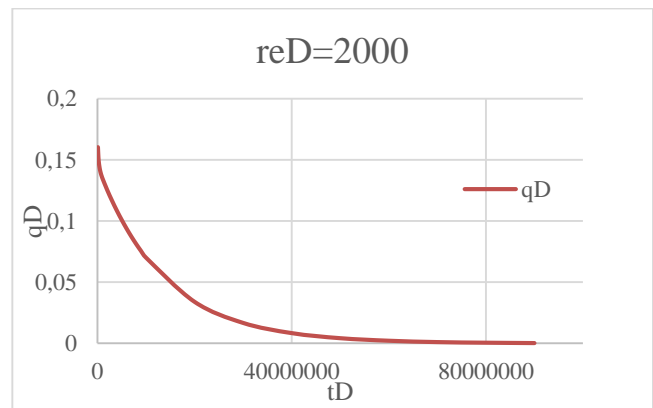


Figure 6. A graph of q_D versus t_D at $r_{eD} = 2000$ under “Closed” boundary condition

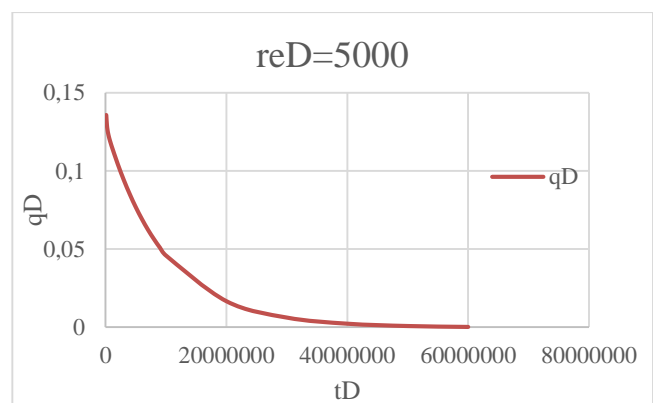


Figure 7. A graph of q_D versus t_D at $r_{eD} = 5000$ under “Closed” boundary condition

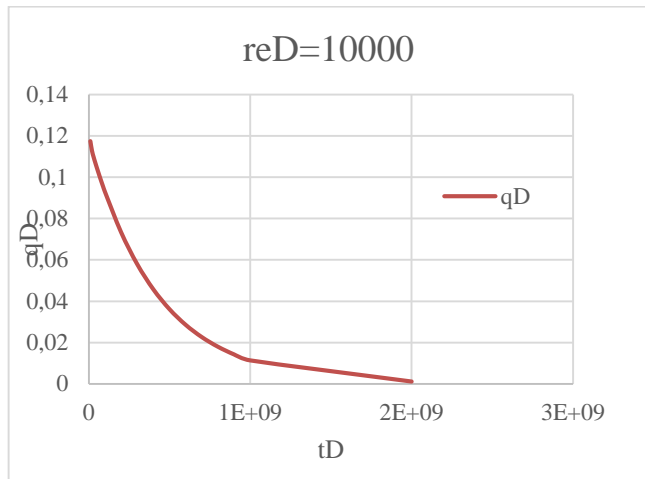


Figure 8. A graph of q_D versus t_D at $r_{eD} = 10000$ under “Closed” boundary condition

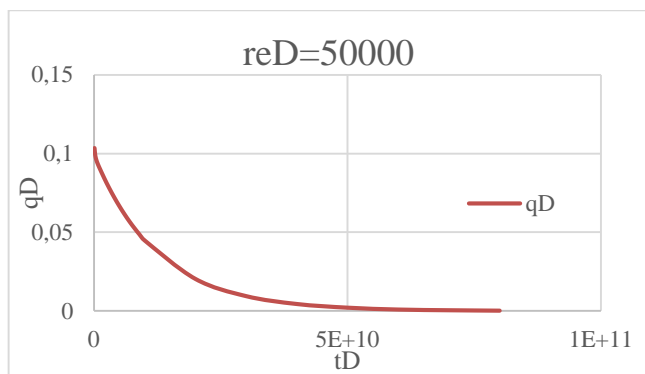


Figure 9. A graph of q_D versus t_D at $r_{eD} = 50000$ under “Closed” boundary condition

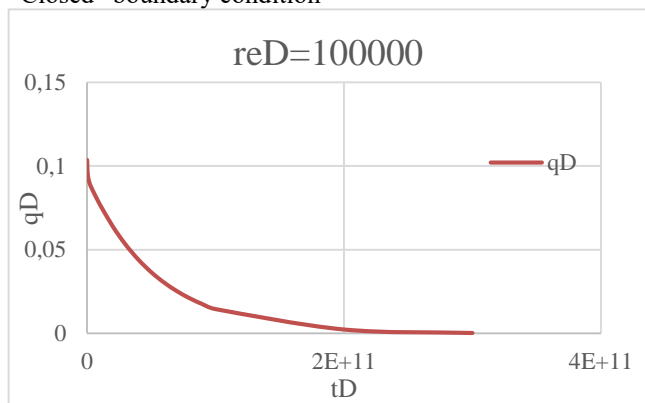


Figure 10. A graph of q_D versus t_D at $r_{eD} = 100000$ under “Closed” boundary condition

From the graphs in Figures 1 to 12, It has been found that the graph did not start at 0 dimensionless time. The reservoir will behave as though it is infinite in its capacity when it is opened. At these times, the operation of the reservoir is different from its performance when it was bounded in size. Therefore, these regions were not captured throughout this stage of the investigation. The reservoir now operates as though there is no

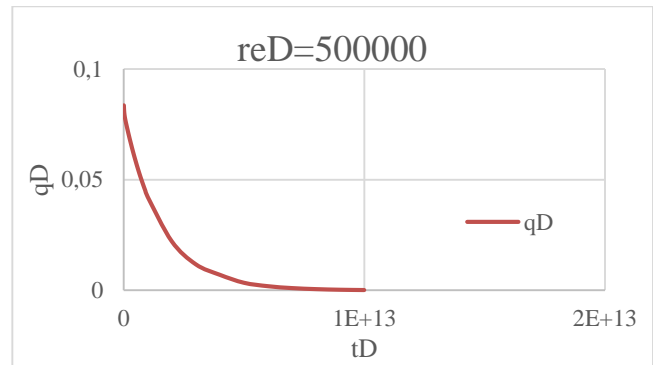


Figure 11. A graph of q_D versus t_D at $r_{eD} = 500000$ under “Closed” boundary condition

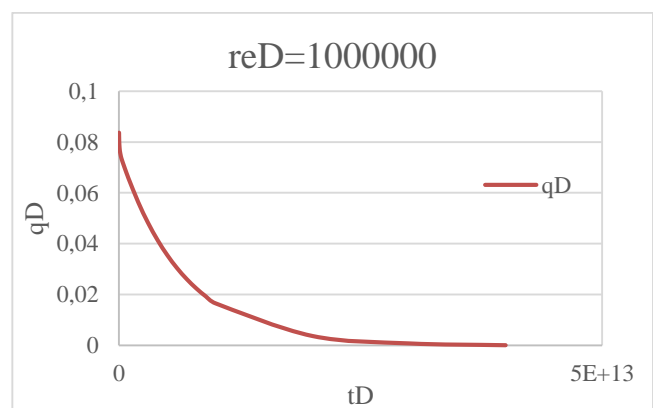


Figure 12. A graph of q_D versus t_D at $r_{eD} = 1000000$ under “Closed” boundary condition

fluid inflow when the outer boundary of the formation observes the pressure disturbance. The reservoir's dimensionless production rate begins to decline as a result. At the early stages of the regime, the rate of decline is considerable, but it eventually becomes steady.

Also, Figs. 13 to 22 shows graphs of dimensionless cumulative production relative to dimensionless time for varying dimensional radial displacement of from 20 to 50,000. From all the graphs in Figs. 13 to 22, it was discovered that the flow crosses the closed boundary regime, there is a linear increase in the cumulative production whenever dimensionless time evolves. Thereafter,

the dimensionless cumulative production becomes asymptotically constant with a very slight increase as the dimensionless time increases. This continues throughout this flow regime. This is simply because there is no flow

into the reservoir as the boundaries are closed. In this flow regime, we can say that the rate at which cumulative production increases, is constant.

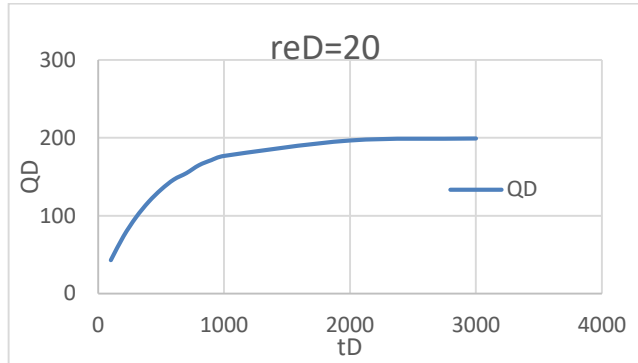


Figure 13. A graph of Q_D versus t_D at $r_{eD} = 20$ under "Closed" boundary condition

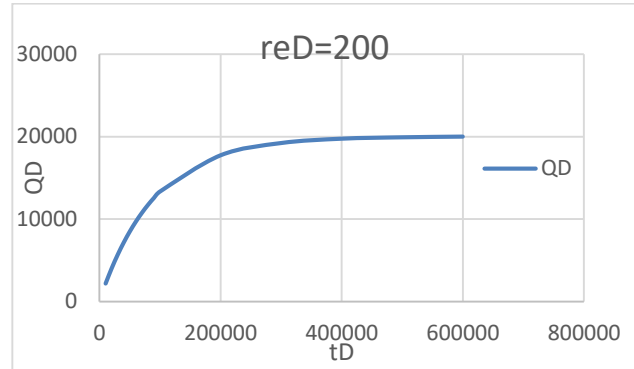


Figure 16. A graph of Q_D versus t_D at $r_{eD} = 200$ under "Closed" boundary condition

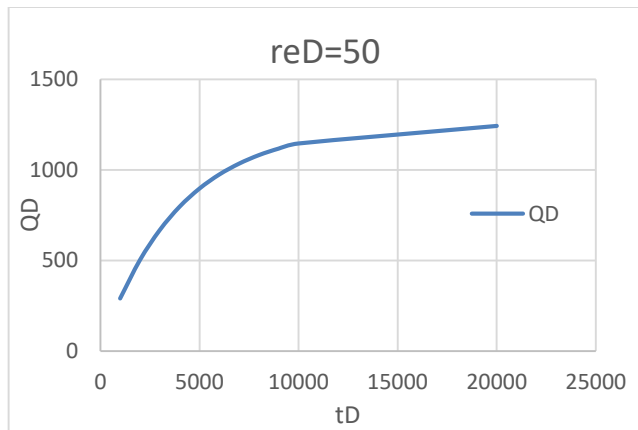


Figure 14. A graph of Q_D versus t_D at $r_{eD} = 50$ under "Closed" boundary condition

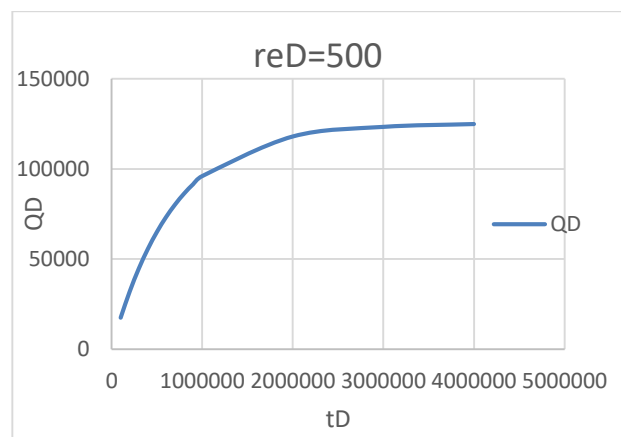


Figure 17. A graph of Q_D versus t_D at $r_{eD} = 500$. under "Closed" boundary condition

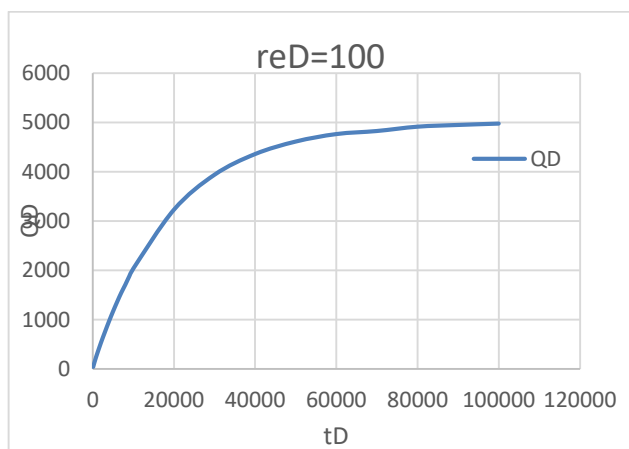


Figure 15. A graph of Q_D versus t_D at $r_{eD} = 100$ under "Closed" boundary condition

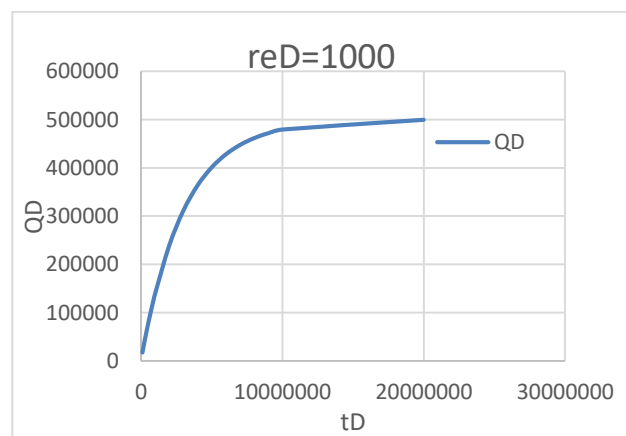


Figure 18. A graph of Q_D versus t_D at $r_{eD} = 1000$ under "Closed" boundary condition

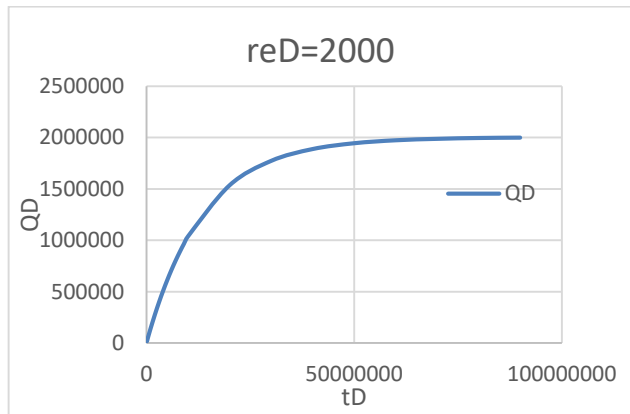


Figure 19. A graph of Q_D versus t_D at $r_{eD} = 2000$ under “Closed” boundary condition

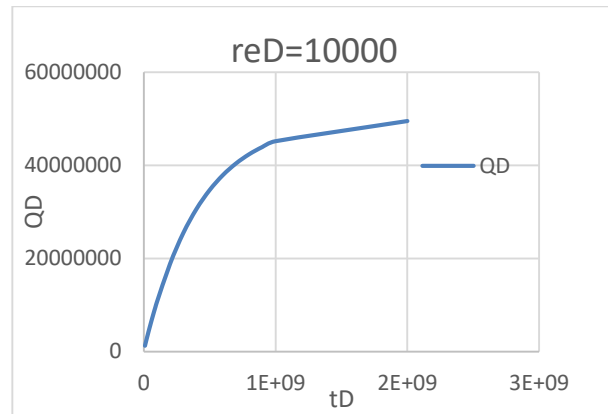


Figure 21. A graph Q_D of versus t_D at $r_{eD} = 10000$ under “Closed” boundary condition

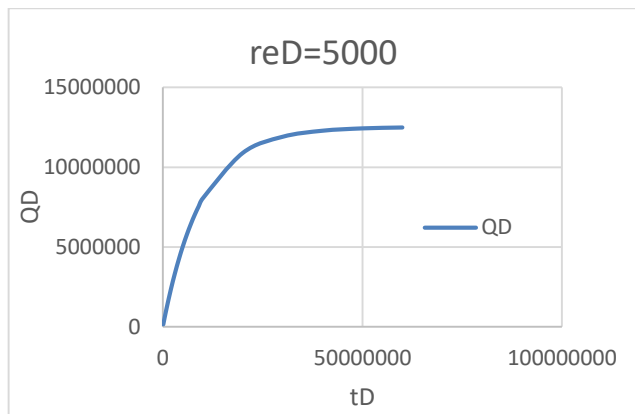


Figure 20. A graph of Q_D versus t_D at $r_{eD} = 5000$ under “Closed” boundary condition

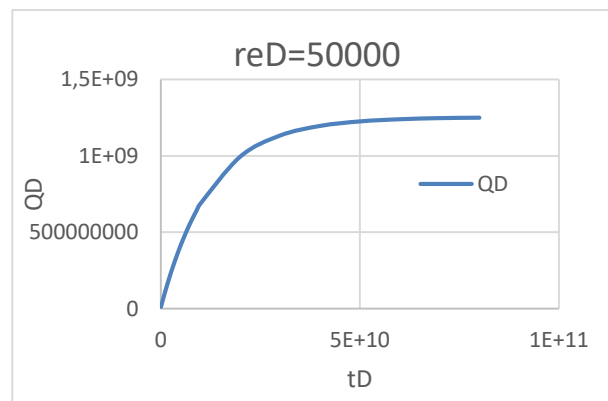


Figure 22. A graph of Q_D versus t_D at $r_{eD} = 50000$ under “Closed” boundary condition.

Table 2. Percentage error between this research study & Christine. (1979) results

$r_{eD} = 20$ $n = 4$			$r_{eD} = 50$ $n = 4$			$r_{eD} = 200$ $n = 4$			$r_{eD} = 500$ $n = 4$		
t_D	Q_D %. Error	q_D %. Error	t_D	Q_D %. Error	q_D %. Error	t_D	Q_D %. Error	q_D %. Error	t_D	Q_D %. Error	q_D %. Error
100.0	0.0388	0.0982	1000.0	0.0012	0.0139	10000.0	0.0008	0.0189	100000.0	0.0191	0.2128
200.0	0.0227	0.1223	2000.0	0.0007	0.0179	20000.0	0.0004	0.0189	200000.0	0.0104	0.2462
300.0	0.0170	0.1519	3000.0	0.0005	0.0230	30000.0	0.0003	0.0189	300000.0	0.0075	0.2849
400.0	0.0141	0.1887	4000.0	0.0004	0.0295	40000.0	0.0002	0.0189	400000.0	0.0060	0.3296
500.0	0.0125	0.2340	5000.0	0.0004	0.0387	50000.0	0.0002	0.0189	500000.0	0.0051	0.3817
600.0	0.0114	0.2906	6000.0	0.0003	0.0485	60000.0	0.0002	0.0189	600000.0	0.0046	0.4415
700.0	0.0108	0.3606	7000.0	0.0003	0.0620	70000.0	0.0002	0.0189	700000.0	0.0042	0.5113
800.0	0.0101	0.4462	8000.0	0.0003	0.0789	80000.0	0.0001	0.0189	800000.0	0.0039	0.5903
900.0	0.0097	0.5520	9000.0	0.0003	0.1010	90000.0	0.0001	0.0189	900000.0	0.0036	0.6830
1000.0	0.0094	0.6816	10000.0	0.0015	0.1290	100000.0	0.0001	0.0189	1000000.0	0.0035	0.7910
2000.0	0.0169	0.5757	20000.0	0.0013	1.5512	200000.0	0.0002	0.0111	2000000.0	0.0056	3.2609

Table 1. Contd

$r_{eD} = 100$ $n = 4$			$r_{eD} = 1000$ $n = 4$			$r_{eD} = 2000$ $n = 4$		
t_D	Q_D % Error	q_D % Error	t_D	Q_D % Error	q_D % Error	t_D	Q_D % Error	q_D % Error
100	0.0033	0.0413	100000	0.0081	0.0891	100000	0.0813	0.0891
200	0.0019	0.0460	200000	0.0043	0.0941	200000	0.0435	0.0940
300	0.0014	0.0487	300000	0.0030	0.0976	300000	0.0303	0.0968
400	0.0011	0.0507	400000	0.0023	0.1009	400000	0.0235	0.0989
500	0.0009	0.0522	500000	0.0019	0.1042	500000	0.0193	0.1004
600	0.0008	0.0534	600000	0.0016	0.1077	600000	0.0165	0.1017
700	0.0007	0.0545	700000	0.0014	0.1112	700000	0.0144	0.1029
800	0.0006	0.0554	800000	0.0012	0.1148	800000	0.0129	0.1039
900	0.0005	0.0562	900000	0.0011	0.1186	900000	0.0116	0.1048
1000	0.0005	0.0569	1000000	0.0010	0.1226	1000000	0.0107	0.1057
2000	0.0013	0.0619	2000000	0.0009	0.1691	2000000	0.0057	0.1139
3000	0.0009	0.0655	3000000	0.0007	0.2346	3000000	0.0040	0.1225
4000	0.0007	0.0690	4000000	0.0006	0.3240	4000000	0.0031	0.1318
5000	0.0006	0.0727	5000000	0.0005	0.4466	5000000	0.0026	0.1417
6000	0.0005	0.0765	6000000	0.0005	0.6134	6000000	0.0023	0.1524
7000	0.0005	0.0805	7000000	0.0005	0.0840	7000000	0.0020	0.1640

Table 1. Contd

$r_{eD} = 5000$ $n = 4$			$r_{eD} = 10000$ $n = 4$			$r_{eD} = 50000$ $n = 4$		
t_D	Q_D % Error	q_D % Error	t_D	Q_D % Error	q_D % Error	t_D	Q_D % Error	q_D % Error
100000	0.0146	0.1053	10000000	0.0114	0.0365	1E+08	0.0130	0.0138
200000	0.0077	0.1103	20000000	0.0060	0.0380	2E+08	0.0068	0.0143
300000	0.0053	0.1131	30000000	0.0041	0.0390	3E+08	0.0046	0.0146
400000	0.0040	0.1152	40000000	0.0031	0.0400	4E+08	0.0035	0.0148
500000	0.0033	0.1168	50000000	0.0025	0.0410	5E+08	0.0028	0.0150
600000	0.0028	0.1183	60000000	0.0021	0.0419	6E+08	0.0024	0.0151
700000	0.0024	0.1197	70000000	0.0019	0.0429	7E+08	0.0021	0.0152
800000	0.0021	0.1210	80000000	0.0016	0.0440	8E+08	0.0018	0.0154
900000	0.0019	0.1223	90000000	0.0015	0.0450	9E+08	0.0016	0.0155
1000000	0.0017	0.1236	1E+08	0.0013	0.0461	1E+09	0.0015	0.0156
2000000	0.0030	0.1369	2E+08	0.0008	0.0584	2E+09	0.0008	0.0169
3000000	0.0021	0.1518	3E+08	0.0006	0.0740	3E+09	0.0005	0.0183
4000000	0.0017	0.1682	4E+08	0.0005	0.0937	4E+09	0.0004	0.0198
5000000	0.0014	0.1865	5E+08	0.0004	0.1187	5E+09	0.0003	0.0215

6000000	0.0012	0.2067	6E+08	0.0004	0.1501	6E+09	0.0003	0.0232
7000000	0.0011	0.2292	7E+08	0.0004	0.1895	7E+09	0.0003	0.0252
8000000	0.0010	0.2539	8E+08	0.0003	0.2389	8E+09	0.0002	0.0272
9000000	0.0009	0.2816	9E+08	0.0003	0.3012	9E+09	0.0002	0.0295
10000000	0.0009	0.3122	1E+09	0.0003	0.3783	1E+10	0.0002	0.0319
20000000	0.0013	0.8617	2E+09	0.0003	0.3909	2E+10	0.0001	0.0704

The obtained results from this investigation have been found to correspond with those already in existence in literature. A table of percentage error between the FEM solutions & the Christine

(1979) solutions was generated in order to assess the level of accuracy. The result from the comparison was shown in Table 2.

3.1. Numerical Convergence Analysis

To verify the numerical reliability of the finite element solution of the radial diffusivity equation under a no flow outer boundary condition, a convergence analysis was performed. The assessment focuses on the asymptotic behaviour of the numerical solution as the dimensionless time increases toward the pseudo-steady-state regime, where the solution is expected to become time independent. Let $Q^D(t^D)$ denote the dimensionless numerical quantity of interest obtained from the finite element computation, such as the dimensionless pressure response or production-related

variable reported in this study. Convergence is assessed using a successive relative difference defined as

$$C(t_k^D) = \frac{Q^D(t_k^D) - Q^D(t_{k-1}^D)}{Q^D(t_k^D)} \quad (20)$$

Where t_k^D and t_{k-1}^D are two consecutive dimensionless times. A decreasing value of $C(t^D)$ indicates that the numerical solution is approaching a stable limiting solution.

Table 3. Convergence Analysis

Dimensionless Time (t^D)	Numerical Result (Q^D)	Successive Difference	Convergence Indicator $C(t^D)$
10^2	0.8729		
10^3	0.9217	0.0488	5.29×10^2
10^4	0.9462	0.0245	2.59×10^2
10^5	0.9581	0.0119	1.24×10^2

The results in Table 3. shows a clear and monotonic decrease in the convergence indicator as the dimensionless time increases from 10^2 to 10^5 . This behaviour confirms that the numerical

solution stabilises progressively and approaches a limiting pseudo steady state solution, as expected for a reservoir governed by a no flow outer boundary condition.

4. Conclusion

For the diffusivity equation in the pseudo-steady state flow regime, we have developed finite element-based models in this study. The production rate and cumulative production for various radii and timeframes were evaluated using the results. This research leads us to the conclusion that, given the reservoir's rock and fluid properties, one may predict the reservoir's production rate and cumulative production.

By comparing the results with those from the exact differential equation solution and those that have already been published in the literature, the accuracy of the results has been confirmed. The results of this investigation show a strong positive correlation with those found in the literature.

References

- [1] T. Ahmed, and P. McKinney, Advanced reservoir management engineering, *Gulf Professional Publishing, Oxford*, 2nd ed., 2011, ISBN: 9780123855480.
- [2] H.S. Carslaw, and J.C. Jaeger *Conduction of Heat in Solids*, Oxford: Clarendon Press, 522 pages ISBN: 9780198533689, 1986.
- [3] W.J. Lee, and R.A. Wattenbarger *Gas reservoir engineering*, SPE Textbook Series, 5. Society of Petroleum Engineers, p. 349, 1996.
- [4] C. Chakrabarty, S. Ali and W. Tortike *Analytical solutions for radial pressure distribution* including the effects of the quadratic gradient term. *Water Resour Res*, 29(4), p. 1171–1177, 1993.
- [5] W.J. Lee, “Pressure transient testing part 9. Production engineering methods”, In: *Development Geology Reference Manual. AAPG Methods in Exploration No. 10*, Tulsa, OK, p. 477–481, 1992.
- [6] A. Van Everdingen, “The skin effect and its influence on the productive capacity of a well”, *J Petrol Techn.*, 5(06) p. 171–176, 1953.
- [7] S. Braeuning, T.A. Jelmert, and S.A. Vik, “The effect of the quadratic gradient term on variable-rate well-tests”, *J. Petrol Sci. Eng.*, 21(3) p. 203–222, 1998.
- [8] Y. Wang, and M.B. Dusseault, “The effect of quadratic gradient terms on the borehole solution in poroelastic media”, *Water Resour Res* 27(12) p. 3215–3223, 1991.
- [9] P. Couto, and M.D. Marsili, A general analytic solution for the multidimensional hydraulic diffusivity equation by integral transform technique, Rio de Janeiro, Brazil, OTC, p. 29 – 31, 2013.
- [10] Y.S. Wu, and J. A Li, generalised framework model for the simulation of gas production in unconventional gas reservoirs. SPE, 163609, 2014.
- [11] A. Reza, M. Mohamad, and S. Zahra, “Parametric analysis of diffusivity equation in oil reservoirs”, *J Petrol Explor. Prod. Technol.*, 6, pp. 1-11, 2016.
- [12] X. u. Yu, K. Regenauer-Lieb, F.-B. Tian, “Effects of surface roughness and derivation of scaling laws on gas transport in coal using a fractal-based lattice Boltzmann method”, *Fuel*, 259 p. 116229, 10.1016/j.fuel.2019.116229, 2020.
- [13] M.M. Rahaman, H. M. Sikdar, B. Hossain, M.A. Rahaman, M. Jamal, “Numerical Solution of Diffusion Equation by Finite Difference Method”, *IOSR Journal of Mathematics (IOSR-JM, Vol. 11(6) Ver. IV PP 19-25*, 2015.
- [14] D. Han, and S. Kwon, “Application of machine learning method of data-driven deep learning model to predict well production rate in the shale gas reservoirs”, *Energies*, 14(12) 3629, p. 1 - 24, <https://doi.org/10.3390/en14123629>, 2021.
- [15] W. M. Charles “Laplace Transform Methods for Transient Diffusion; or, Some Good Questions from Ralph White. *Journal of The Electrochemical Society*”, 170 093509, 245th ECS Meeting, 2023.
- [16] A. S. Farman, N. Kamran, S. Kaimal, A. Thabet, “Numerical modelling of advection diffusion equation using Chebyshev spectral collocation method and Laplace transform”, *Results in Applied Mathematics*, Science Direct, Elsevier, Vol (21), 100420, 2024.
- [17] D. Sauli, N. Gjika, E. Xhafaj, R. Kosova, E. Zeqo, “Analyzing Oil Reservoir Dynamics: Leveraging Separated Variable Solution of Radial Diffusivity Equation with Constant Bottom Flux”, *Mathematical Modelling of Engineering Problems*, Vol. 11(12) p. 3300-3306, 2024
- [18] W. Ratawessanun, K. D. Gisolf, A., Millot, P., Cavalleri, C., Gao, B. “Pioneer in integrated workflow for deep transient testing (DTT) from interpretation to forecast”, In *International Petroleum Technology Conference*, Bangkok, Thailand. <https://doi.org/10.2523/IPTC-22964-MS>, 2023.
- [19] L. O. Pelisoli, R. M. Cotta, C. P. Naveira-Cotta, P. Couto, Three-dimensional transient flow in heterogeneous reservoirs: Integral transform solution of a generalized point-source problem. *Journal of Petroleum Science and Engineering*, Vol. 211, 109976, 2022.
- [20] F. B. Fernandes, A. M. Braga, B. Serra de A. L. Souza, A. C. Soares, Analytical model to effective permeability loss monitoring in hydraulically fractured oil wells in pressure-sensitive reservoirs”, *Geoenergy Science and Engineering*, Vol. 221, 111248, 2023.
- [21] K. Qiu “A practical analytical model for performance prediction in unconventional gas reservoir”, *Front. Earth Sci.* vol. 11, 1143541, 2023.